J Mater Sci (2019) 54:8971–8983

Composites

Tailoring the mechanical and thermal properties of polylactic acid-based bionanocomposite films using halloysite nanotubes and polyethylene glycol by solvent casting process

Swati Sharma[1], Anshu Anjali Singh[1], Abhijit Majumdar[1], and Bhupendra Singh Butola[1,*]

[1] *Department of Textile Technology, Indian Institute of Technology Delhi, Hauz Khas, New Delhi 110016, India*

Received: 14 December 2018
Accepted: 7 March 2019
Published online: 12 March 2019

ABSTRACT

The inherent brittleness of PLA is a major challenge for its use in various applications. In this study, the effect of incorporation of halloysite nanotube (HNT) and polyethylene glycol (PEG) on mechanical and thermal properties of polylactic acid (PLA) was investigated. Various concentrations of PEG-600 and HNT were used with PLA, and films were prepared by solvent casting method. Mechanical, morphological, and thermal properties of these composite films were investigated to study the effect of PEG and HNT on the properties of PLA. Addition of PEG increased elongation at break, but reduced the tensile strength. However, addition of HNT in PLA/PEG compensated the fall in tensile strength. Addition of 3 wt% HNT into PLA blend involving 5 wt% PEG increased its elongation at break by 640% and tensile strength by 22%, while no significant change in Young's modulus was observed. Dynamic mechanical thermal analysis (DMTA) showed significant improvement in storage modulus of PLA/PEG/HNT films in the rubbery region. Glass transition temperature decreased for the PEG-plasticized films, while the crystallinity improved as compared to neat PLA. Thermal stability of PLA/PEG/HNT films was higher than those of PLA, PLA/PEG, and PLA/HNT films. The degree of crystallinity obtained using X-ray diffraction analysis showed good agreement with that determined from differential scanning calorimetry (DSC).

Address correspondence to E-mail: bsbutola@textile.iitd.ac.in

https://doi.org/10.1007/s10853-019-03521-9

Introduction

With a plethora of innovations and excessive dependence on non-biodegradable materials like conventional plastics, humans have depleted the natural resources at a rigorous pace, causing major environmental issues like pollution escalation and dumping space congestion. Use of biodegradable and renewable raw materials has become the necessity of the time, and biopolymers like polylactic acid (PLA) offer a green and sustainable solution to such environmental issues with attractive mechanical and thermal properties [1]. Owing to its numerous advantages, PLA's acceptance in various fields like medicines, packaging, agriculture, and automotive is increasing day by day [2]. Despite having useful properties like high tensile strength comparable to other commodity polymers (e.g., polyesters, polypropylene, PVC, etc.), the application of PLA in biocomposite field is limited due to its low impact strength and low flexibility or ductility [3, 4]. Thus, there is an exigent need to balance the stiffness–toughness properties of PLA without impacting its biocompatibility and biodegradability and make it more acceptable for various applications.

Several approaches have been explored by the scientists and researchers to improve the toughness of the PLA, for example grafting with suitable polymers, physical blending with plasticizers etc. [2, 5–10]. Commonly used plasticizers to counter the brittle behavior of PLA are polyethylene glycol (PEG) [5], polypropylene glycol (PPG) [6], epoxidized soybean oil (ESO), epoxidized palm oil (EPO) [7]. Jacobson and Fritz [8] used three different plasticizers (PEG-600, partial fatty acids, and glucose monoesters) for PLA and found that the glass transition temperature (T_g) of PLA dropped with slight or no change in melting point. Also, the tensile strength and tensile modulus decreased with the addition of plasticizers, while elongation at break increased drastically. The principal disadvantage of using these plasticizers is a consequent decrease in the tensile strength of toughened PLA. Thus, to balance the strength and toughness of PLA, a synergistic approach is required. One such alternative technique to achieve high strength and modulus is to add nanofiber or nanoparticle while manufacturing plasticized PLA composites films. Shi et al. [9] studied the effect of plasticizer (PEG) and nanofillers (precipitated calcium carbonate, HNT, LAK) simultaneously in the PLA matrix. They found that the nanofillers acted as the reinforcement, while the plasticizer was effective in improving the PLA chain mobility. Mohapatra et al. [10] also studied the effect of PEG on PLA and its nanocomposites and found that the addition of nanofillers (organoclay) in PLA/PEG matrix improved the tensile and impact properties. Use of different nanofillers like nanoclay, zinc oxide nanoparticles, carbon nanotubes (CNTs), graphene nanoplatelets (GNPs), cellulose nanofibers (CNFs) is currently being practiced to improve the mechanical and thermal properties of PLA [11–14]. Among all other nanofillers, nanoclays have drawn a lot of attention among researchers due to their chemical structure, mechanical properties, and cost-effectiveness as they are copiously available on earth's surface.

Halloysite nanotubes (HNTs), a potential nanofiller candidate, have large aspect ratio, high mechanical strength, good biocompatibility, and low cost. HNTs are one-dimensional naturally occurring aluminosilicates with a tubular structure. Their molecular formula is Al2Si2O5(OH)4·nH2O which is similar to that of hydrated kaolinite [15]. HNTs are relatively hydrophobic in comparison with other nanoclays as it contains less hydroxyl (–OH) groups on the surfaces, and its outer surface primarily comprises a siloxane with a few silanols/aluminols exposed on the edges. Therefore, it is easy to disperse HNT in a nonpolar polymer just by the application of shear. However, the inherent hydrophobicity of HNTs does not provide sufficient interfacial adhesion in polymer nanocomposites [16]. Use of HNTs as a nanofiller in polymers improves the mechanical and thermal properties significantly [17, 18]. Dong et al. [19] have prepared PLA/HNT composites mats using electrospinning and observed an improvement in tensile strength and modulus with improved thermal stability. Esma et al. [20] reported the use of PEG and TPU as a plasticizer for the processing of the PLA/HNT nanocomposites by melt compounding. They found that TPU showed better compatibility with PLA than PEG and improved the flexibility of nanocomposites without compromising the strength.

Limited work has been reported on the use of HNT as reinforcement for PLA nanocomposites, though it is a very promising nanofiller. To the best of our knowledge, no work has been reported till date on the processing of PLA/HNT nanocomposites with PEG by solvent casting at room temperature. In this

study, composite films of PLA have been prepared by solvent casting technique, where HNT acted as a reinforcement and PEG as a plasticizer. Effect of different combinations of HNT and PEG concentrations on the morphological, mechanical, and thermal properties of PLA nanocomposite films was studied.

Materials and methods

Materials

Polylactic acid (PLA) 4043D in the form of pellets with 94% L-lactic acid and 6% D-lactic acid content [21] was supplied by NatureWorks Co. Ltd. Coimbatore, India. Halloysite nanotube (HNT) was purchased from Natural Nano Inc. USA. Polyethylene glycol (PEG, molecular weight = 600) was procured from Sigma-Aldrich. Dichloromethane (DCM) of AR grade was purchased from Fischer Scientific.

Preparation of PLA and PLA-based nanocomposite films

Solvent casting method, with dichloromethane (DCM) as solvent, has been used for the preparation of samples. Four different concentrations of PEG-600 (3, 5, 10, and 20 wt% of PLA) have been used to improve the ductility of PLA. Halloysite nanotube (HNT) of different concentrations ranging from 3 to 20% (wt% of PLA) was used as a nanoreinforcement to improve the mechanical and thermal properties of PLA. For the preparation of neat PLA films, pellets were first dissolved in dichloromethane (DCM) at room temperature using magnetic stirrer for 12 h, and the solution was then cast on a glass petri dish for drying in ambient atmosphere. Plasticizers and/or nanoreinforcement was mixed in the solution of PLA and DCM for the preparation of PLA films with PEG and/or HNT. The obtained solutions were then cast on a glass petri dish and dried in the ambient atmosphere in a fume hood followed by further drying in a vacuum oven for 40 h at 40 °C.

Characterization methods

Tensile testing

Tensile testing of all the samples was carried out as per ASTM D882 using a universal tensile testing machine (Instron 3365). Rectangular-shaped specimens of each sample having a width of 10 mm were tested at a crosshead speed of 10 mm/min with a gauge length of 50 mm. The mean value of the five-test specimen for each sample was recorded as a result.

Morphology characterization

Scanning electron microscopy (SEM) was carried out on the tensile fractured samples using an LEO 982 (Zeiss) SEM operating at 5 kV. The samples were coated with gold before the analysis.

Dynamic mechanical analysis (DMA)

DMA of neat PLA, PLA/PEG, PLA/HNT, and PLA/PEG/HNT was performed to study the variation in storage modulus and loss factor with respect to temperature. The analysis was carried out on DMA Q800 using rectangularly shaped specimen in tensile mode at a constant strain of 0.05% and a constant frequency of 1 Hz. Storage and loss modulus were recorded as a function of temperature from 27 to 135 °C at a heating rate of 2 °C/min.

Differential scanning calorimetry

Thermal properties of the neat PLA and PLA/PEG, PLA/HNT, and PLA/PEG/HNT were studied using differential scanning calorimetry (DSC Q 2000, TA) under nitrogen flow. The samples weighing 2.5 mg were heated gradually in aluminum crucibles at a heating rate of 10 °C/min from 30 to 200 °C and kept at 200 °C for 5 min to remove the effect of the sample's previous history. The samples were then cooled to 0 °C at a cooling rate of 5 °C/min and heated again to 200 °C at 10 °C/min. In this study, glass transition temperature (T_g), melting temperature (T_m), and degree of crystallinity (χ_c) were determined from the second heating scans. The degree of crystallinity was calculated using Eq. 1, where W_f is the weight fraction of the filler, ΔH_m is the enthalpy of melting, and for 100% crystalline PLA, its value is 93 J [10].

$$\%\chi_c = \frac{\Delta H_m}{93(1 - W_f)} \times 100 \quad (1)$$

Thermogravimetric analysis

Thermogravimetric analyses (TGAs) were performed on PerkinElmer 4000 in nitrogen atmosphere. Samples weighing around 7–8 mg were heated in a crucible from room temperature to 600 °C at a heating rate of 10 °C/min, and weight loss of the samples against temperature was plotted.

X-ray diffraction

X-ray diffractograms of film samples were recorded at room temperature using a Rigaku, Ultima IV in reflection mode. The Cu α source was used to carry out the X-ray scans, and 2θ scan data were collected at 0.02°/interval over the 2θ range from 5° to 40°. The scan speed used in performing X-ray diffraction was 3° (2θ)/min. Percentage crystallinity ($\%\chi_c$) of different film samples was calculated using Eq. 2:

$$\%\chi_c = \frac{\text{Area under the peak}}{\text{Total area}} \times 100. \quad (2)$$

Results and discussion

Visual appearance of the films

Figure 1 illustrates the visual appearance of the neat PLA, PLA/PEG, PLA/HNT, and PLA/PEG/HNT films. Neat PLA film is more transparent than the PLA films with PEG and/or HNT additives. Addition of PEG and HNT in PLA makes the films less transparent, and opaqueness of these films further increases with increase in additives concentration. Composite films of PLA/PEG/HNT are the least translucent of all. This decrease in transparency is attributed to the formation of more crystals in plasticized PLA and PLA/HNT nanocomposites compared to neat PLA.

Similar findings were reported by Herrera et al. [22] for PLA plasticized with GTA (glycerol triacetate) and PLA with GTA and CNFs (cellulose nanofibers). It was reported that the PLA-GTA and PLA-GTA-CNF are more crystalline than the neat PLA, thus decreasing the light transmittance and therefore the transparency.

Tensile properties of the films

The tensile properties of the PLA, PLA/PEG, PLA/HNT, and PLA/PEG/HNT films are shown in Table 1, and their corresponding stress–strain curves are shown in Fig. 2. The ultimate tensile strength (UTS), Young's modulus, and % elongation at break of neat PLA films were found to be 47 MPa, 2.4 GPa, and 4.7%, respectively. It can be inferred from Fig. 2a and Table 1 that addition of PEG in PLA decreases the UTS and tensile modulus, while it increases the elongation at break. These changes in tensile properties of PLA can be attributed to the plasticization effect of PEG [5]. After the addition of 20 wt% PEG to PLA (i.e., PLA/PEG20), the elongation at break was

Figure 1 Visual appearance of prepared films.

Table 1 Tensile properties of the prepared samples

Samples	Ultimate tensile strength (MPa)	Tensile modulus (GPa)	Elongation at break (%)
Neat PLA	47.0 (± 2.6)	2.4 (± 0.10)	5 (± 0.4)
PLA/PEG3	31.8 (± 1.1)	1.7 (± 0.03)	70 (± 6)
PLA/PEG5	31.9 (± 1.5)	1.9 (± 0.07)	69 (± 8)
PLA/PEG10	21.2 (± 0.9)	1.2 (± 0.05)	76 (± 13)
PLA/PEG20	20.2 (± 0.7)	1.2 (± 0.02)	159 (± 22)
PLA/HNT3	46.5 (± 0.9)	2.4 (± 0.10)	4 (± 1)
PLA/HNT5	27.8 (± 1.1)	1.5 (± 0.07)	8 (± 1)
PLA/HNT10	40.0 (± 1.4)	2.1 (± 0.10)	5 (± 0.3)
PLA/HNT20	32.9 (± 3.0)	2.2 (± 0.10)	4 (± 1)
PLA/PEG5/HNT3	38.8 (± 1.2)	2.0 (± 0.30)	37 (± 4)
PLA/PEG5/HNT5	30.7 (± 2.3)	2.1 (± 0.10)	40 (± 5)
PLA/PEG5/HNT10	18.6 (± 0.6)	1.0 (± 0.03)	34 (± 2)
PLA/PEG10/HNT10	22.3 (± 1.3)	1.3 (± 0.10)	31 (± 4)
PLA/PEG10/HNT20	23.4 (± 1.2)	1.6 (± 0.20)	33 (± 6)
PLA/PEG20/HNT10	11.2 (± 0.7)	1.0 (± 0.08)	60 (± 15)

Standard deviation in parentheses

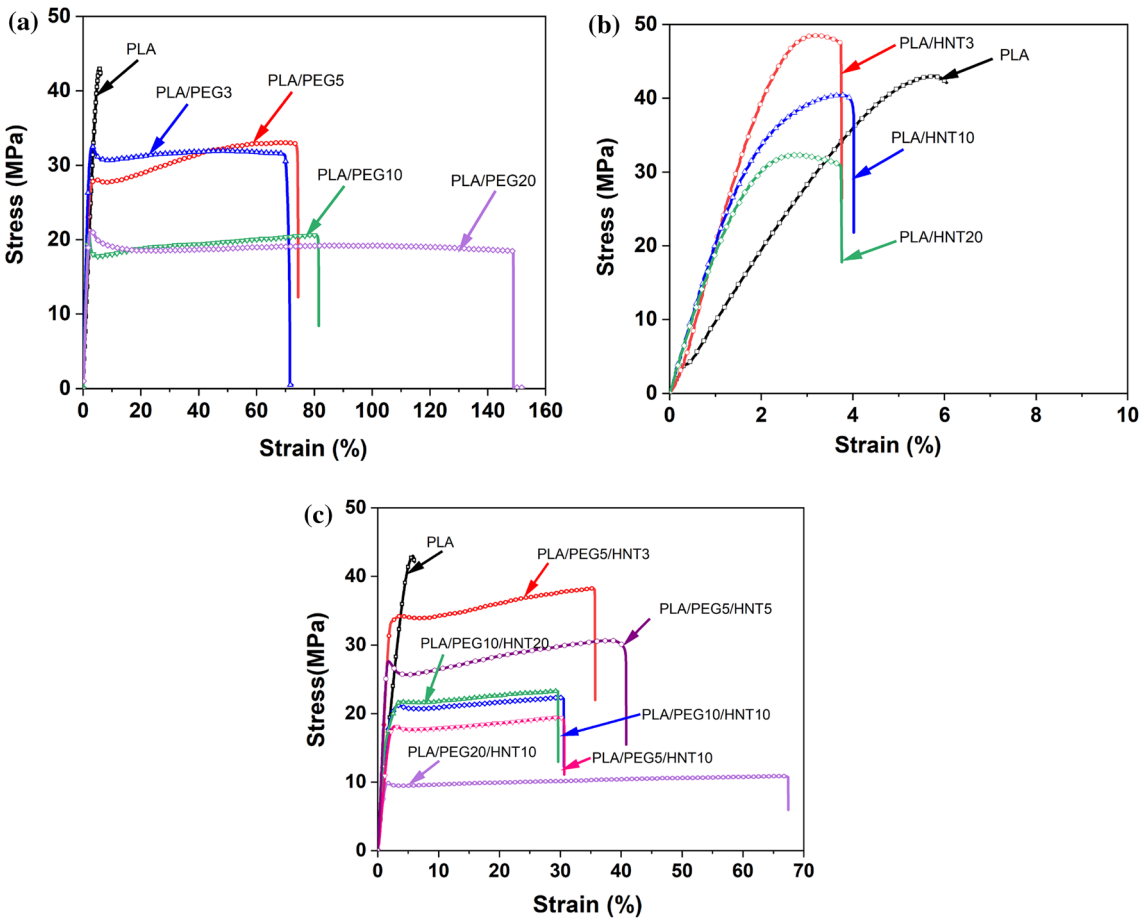

Figure 2 Stress–strain curve of **a** PLA and PLA/PEG film, **b** PLA and PLA/HNT film, and **c** PLA and PLA/PEG/HNT film.

found to be 158%, which is approximately 30 times higher than that of neat PLA (Table 1). However, negligible difference in the tensile properties was observed between the PLA/PEG3 and PLA/PEG5, although the presence of 3 and 5 wt% PEG in PLA improved the toughness of PLA. Jacobsen et al. [8] reported in their study that the addition of 2.5 and 5 wt% PEG-1500 in PLA does not show a significant change in the tensile properties, and the main effect can be seen above 5 wt% concentration of PEG-1500.

Further, it can be seen from Fig. 2b and Table 1 that the addition of HNT does not significantly improve the tensile properties of PLA. Although PLA with 3 wt% of HNT showed no significant variation in tensile properties, when the concentration of HNT increased to 5 wt%, the tensile strength and modulus decreased, while the elongation at break improved (Table 1). Although the addition of reinforcements in polymer decreases the elongation at break [23], the increase in elongation in PLA/HNT5 might be due to the slippery effect of the nanotubes on the PLA matrix and/or crazing effect for this composition [22]. It has been reported that the addition of nanoclay increased the toughness of PLA by acting as a bridge between the cracks at ~ 5 wt%, but as the concentration increased to 10 wt%, the toughening effect disappeared due to the agglomeration [20]. Interestingly, when the amount of HNT incorporated was above 5 wt%, although tensile strength and tensile modulus decreased, no significant change in elongation at break was detected [24].

Figure 2c represents the stress–strain curve of the PLA/PEG/HNT composite films, and the corresponding values of tensile properties are reported in Table 1. It can be inferred from Table 1 that the incorporation of 3 wt% HNT into PLA/PEG5 improves the tensile strength, while the elongation at break was decreased, indicating good interfacial adhesion and dispersion of HNT in PLA/PEG. Further, the addition of 5, 10, and 20 wt% HNT in PLA/PEG5 (i.e., PLA/PEG5/HNT5, PLA/PEG5/HNT10, and PLA/PEG5/HNT20) decreased elongation at break, tensile strength, and tensile modulus except for PLA/PEG5/HNT5, which had tensile properties similar to those of PLA/PEG5. The lower tensile strength of PLA/PEG/HNT nanocomposites at higher HNT wt% is due to the agglomeration of nanoreinforcement in the composites, resulting in poor stress transfer. As shown in Table 1, when PEG concentration was increased to 10 wt% in the nanocomposites having 10 and 20 wt% HNT (i.e., PLA/PEG10/HNT10 and PLA/PEG10/HNT20), slight improvement in the tensile strength and tensile modulus was observed, while the elongation at break decreased as compared to PLA/PEG10. This indicates that good dispersion of HNT was achieved at 10 wt% concentration of PEG which resulted in higher tensile properties due to good stress transfer. But, further increase in PEG concentration to 20 wt% (i.e., PLA/PEG20/HNT10) decreased the overall mechanical properties of the nanocomposite. However, the elongation at break of PLA/PEG20/HNT10 is higher than that of PLA/HNT10 by 1200% due to the plasticizing effect of PEG. Similar trends were also reported by the Pillin et al. [25] and Ozdemir et al. [26], and according to them, poor dispersion of PEG in the PLA at higher concentrations may be responsible for poor mechanical properties of PEG-plasticized composites.

Morphology of the films

Figure 3a–d shows the SEM images of tensile fractured surface of neat PLA and PLA/PEG samples. It can be seen in Fig. 3a that the surface of neat PLA is smooth indicating its brittle nature [22]. However, the addition of PEG in PLA results in large plastic deformation (Fig. 3b–d), which increases the surface roughness. Voids formation due to the plasticization of PLA can be seen in the tensile fractured surface of PLA/PEG20 in Fig. 3d. Similar morphology was reported in the literature when PLA had been plasticized with PPG, Boltorn®, and natural rubber [6, 27, 28].

Figure 4a–c shows the SEM images of tensile fractured surfaces PLA/HNT films. The tensile fractured PLA/HNT films have a rough surface, which might be due to the presence of HNT in the PLA. However, this roughness is lower than that of PLA/PEG (Fig. 3b–d), indicating brittle behavior of PLA/HNT. With increase in HNT concentration, the surface became more irregular caused by the agglomeration of HNT and the same is visible in Fig. 4b, c.

Further, Fig. 5a–c shows SEM images of PLA/PEG/HNT composite films, and it can be observed that the surface of the films is more rough and has more voids. This irregular and uneven surface indicates the presence of PEG in the PLA, and the agglomeration of HNT can also be seen at high HNT concentrations.

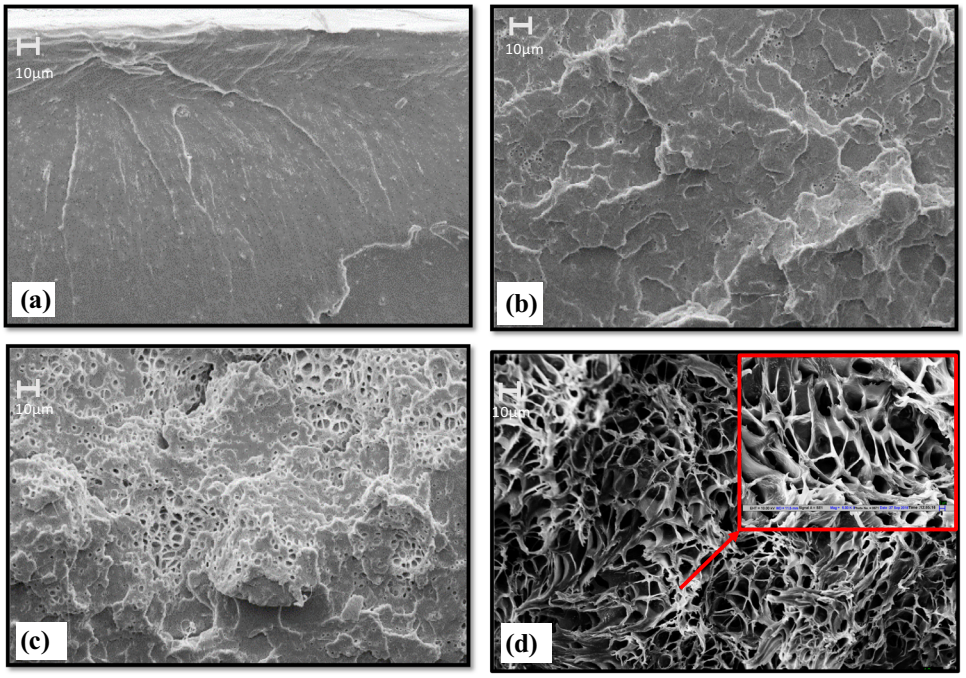

Figure 3 SEM images of the tensile fractured surface of **a** Neat PLA, **b** PLA/PEG5, **c** PLA/PEG10, and **d** PLA/PEG20 films.

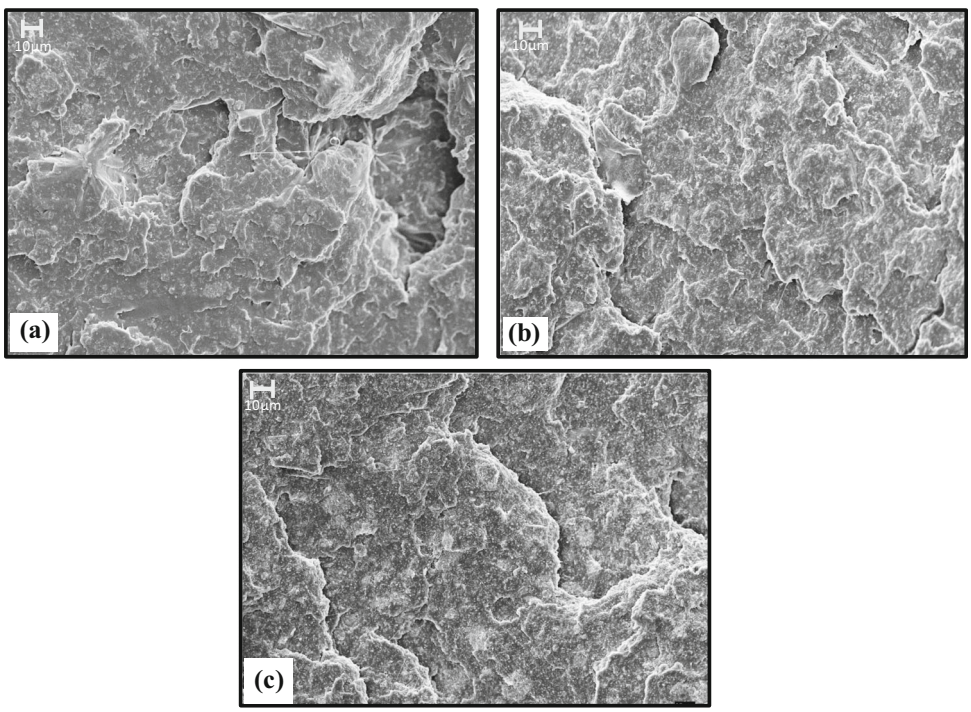

Figure 4 SEM images of the tensile fractured surface of **a** PLA/HNT5, **b** PLA/HNT10, and **c** PLA/HNT20 films.

It can be noticed from Table 1 that there is no significant difference between the elongation at break for PLA/PEG5 and PLA/PEG10. However, the tensile strength and tensile modulus of PLA/PEG5 are significantly higher than that of PLA/PEG10. Owing to the relatively similar tensile properties of PLA/HNT3 and PLA/HNT10, only PLA/HNT10 was considered for the thermo-mechanical and thermal characterizations. Following similar approach PLA/PEG5 and PLA/PEG5/HNT10 were selected for thermo-mechanical and thermal characterization to analyze the effect of additives on PLA in this study.

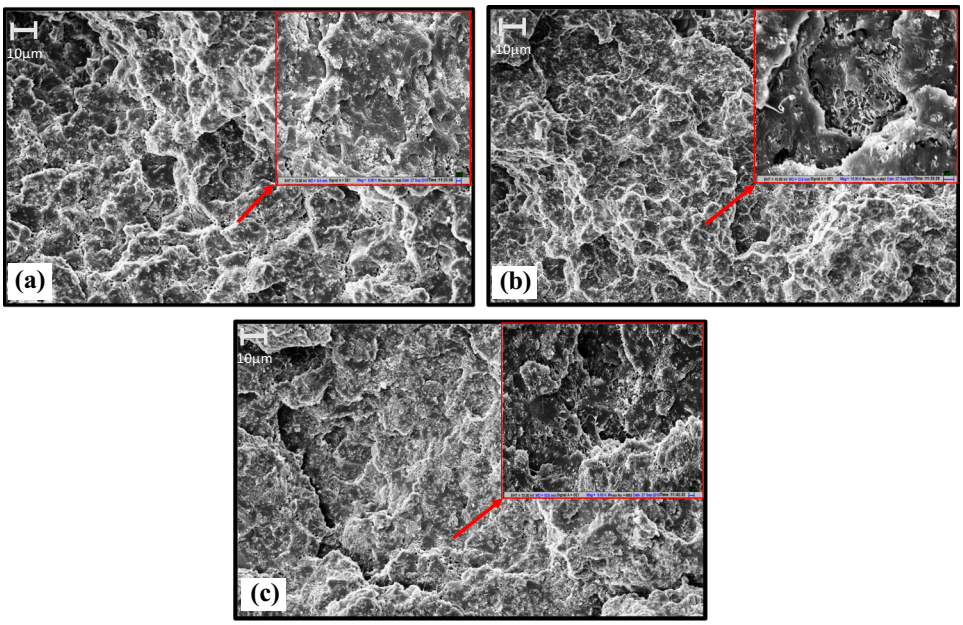

Figure 5 SEM images of the tensile fractured surface of **a** PLA/PEG5/HNT10, **b** PLA/PEG10/HNT10, and **c** PLA/PEG10/HNT20.

Dynamic mechanical analysis (DMA)

Figure 6 shows the variation in storage modulus and Tan delta (δ) for neat PLA, PLA/PEG5, PLA/HNT10, and PLA/PEG5/HNT10 films as a function of temperature. It can be observed that the addition of PEG in the PLA (i.e., PLA/PEG5) changes the storage modulus in both glassy and rubbery regions, and this is attributed to the plasticization effect of PEG on PLA [29]. Compared to neat PLA, the storage modulus of PLA/PEG5 is lower in the glassy region, while the value of the same increases in the rubbery region. The storage modulus at 70 °C for neat PLA and PLA/PEG5 was recorded as 11 and 242 MPa, respectively. A similar trend has been reported in PLA/glycerol triacetate (GTA) blends [30]. The addition of HNT (i.e., PLA/HNT10 and PLA/PEG5/HNT10) did not affect the storage modulus at room temperature. However, storage modulus decreased with increase in temperature and a steep fall was observed around 60–70 °C. This drop in the storage modulus is more prominent for the neat PLA, and this could be attributed to the typical effect of cold crystallization. A mild drop in storage modulus in other composite films indicates a high degree of crystallinity than the neat PLA [31]. Interestingly, it is seen that the storage modulus of PLA/HNT10 and PLA/PEG5/HNT10 has a higher value than the neat PLA in the rubbery region. The storage modulus of PLA, PLA/HNT10, and PLA/PEG5/HNT10 at 70 °C was recorded as 11 MPa, 273 MPa, and 473 MPa, respectively. Of all the samples tested, PLA/PEG5/HNT10 was found to have the highest storage modulus at 70 °C (rubbery region), and this may be attributed to the synergistic effect of PEG and HNT acting as a plasticizer and reinforcement, respectively, and increased the degree of crystallinity [32].

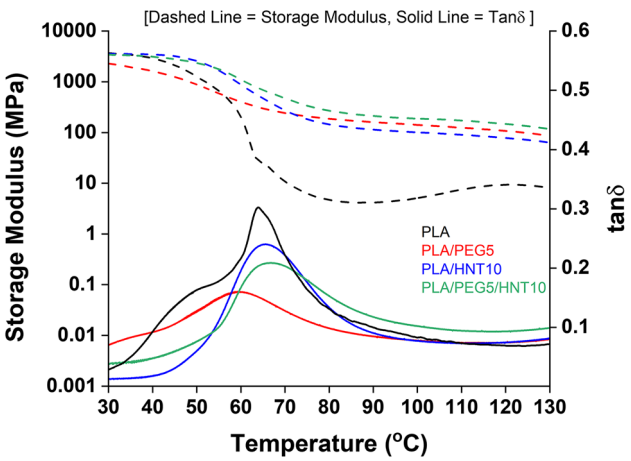

Figure 6 DMA of neat PLA and composite films.

Furthermore, it can also be observed from Fig. 6 that the Tanδ peak shifted slightly to higher temperature for the PLA/HNT10 and PLA/PEG5/HNT10 compared to neat PLA and the amplitude of Tanδ decreased. The Tanδ peak for the PLA, PLA/PEG5, PLA/HNT10, and PLA/PEG5/HNT10 was recorded at 63.7, 59.3, 65.5, and 66.6 °C, respectively. This shift in the Tanδ peak toward higher

temperature for PLA/HNT10 and PLA/PEG5/HNT10 is attributed to the restricted molecular movement, and the decreased intensity indicates the crystal formation and participation of fewer polymer chains in the transition [33]. It has been reported that the decreased amplitude of Tanδ peak could also be attributed to the well-dispersed and distributed nanoreinforcement [30]. Overall, the results indicate that the improvement in the thermo-mechanical properties of the PLA/PEG/HNT is due to the synergistic effect of PEG and HNT.

Differential scanning calorimetry (DSC)

Thermal characterization of PLA, PLA/PEG5, PLA/HNT10, and PLA/PEG5/HNT10 was carried out to analyze the effects PEG and HNT on PLA. DSC thermograms obtained after first and second heating scans of the samples are shown in Fig. 7. Glass transition temperature (T_g), cold crystallization temperature (T_{cc}), melting temperature (T_m), and degree of crystallinity (X_c) of the samples obtained after second heating scan are reported in Table 2. The T_g and T_m of neat PLA films were recorded around 56 and 147 °C, respectively, during the first heating scan and 61 and 149 °C, respectively, during the second heating scan. It can be seen from Fig. 7b that there is no significant change in the T_g in the case of PLA/HNT10, while the same decreases for PLA/PEG5 and PLA/PEG5/HNT10 samples when compared with neat PLA. This shift of T_g to lower temperature can be principally attributed to the increased molecular mobility of chains caused by the plasticization effect of PEG [34, 35].

The double melting peaks can be observed in the second heating scan of PLA/PEG5/HNT10 (Fig. 7b). It was reported that the double melting peak during the second heating scan might be caused by the variation in crystal sizes, after the first heating scan. The imperfect crystals rearrange themselves to form perfect crystal, thus melting slowly at higher temperature forming the shoulder peak [29].

Similar twin peaks were also observed by Silverajah et al. who plasticized PLA with epoxidized palm oil, suggesting that plasticizers affect the crystallization behavior of PLA, resulting in the formation of soft segments and hard segments. These hard and soft segments melt at different temperatures, resulting in twin melting peaks [33].

Table 2 summarizes the effect of plasticizer and nanofiller addition on glass transition temperature, melting temperature, and crystallinity of the PLA. From Fig. 7, it can be seen that in the first heating scan, the T_{cc} is almost absent in all the films, whereas in the second heating scan in the case of PLA/PEG and PLA/PEG/HNT composite films, the T_{cc} is quite prominent, suggesting that the addition of PEG enhances the crystallization capacity of PLA [36].

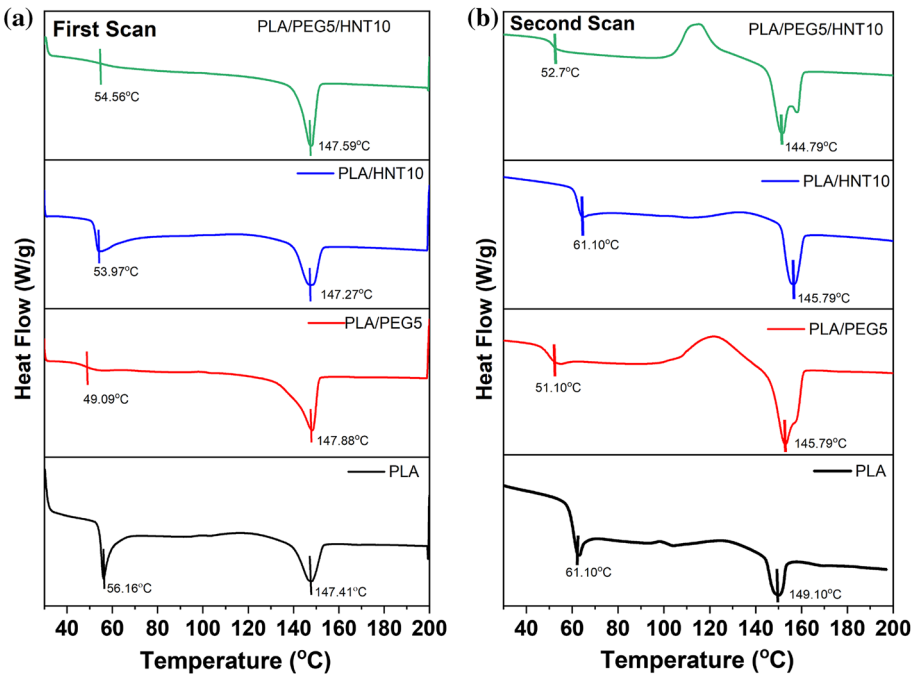

Figure 7 DSC thermograms of PLA and PLA composite films.

Table 2 Characteristic temperature of PLA and its composite from TGA and second heating scan of DSC

Material	DSC			TGA	
	T_g (°C)	T_m (°C)	%X_c	T_{50} (°C)	T_{max} (°C)
PLA	61.10	149.10	3.45	337	346
PLA/PEG5	51.13	145.79	24.33	337	346
PLA/HNT10	61.47	148.24	9.57	352	355
PLA/PEG5/HNT10	52.07	144.10	23.37	366	370

In the case of PLA/HNT composite film, the T_{cc} can be observed, but it is not as prominent as that of PLA/PEG and PLA/PEG/HNT films. The addition of PEG and HNT in the PLA improves the degree of crystallinity when compared with neat PLA. Therias et al. [37] reported that the addition of HNT showed improvement in the crystallization of PLA only at higher concentrations (12 wt%).

Thermogravimetric analysis (TGA)

Thermogravimetric analysis (TGA) was performed to study the effect of PEG and HNT on the thermal degradation behavior of PLA in the inert atmosphere. Figure 8a, b shows the TGA (wt% loss vs. temperature) and derivative thermogravimetric (DTG) (wt%/°C vs. temperature) curves of the PLA, PLA/PEG5, PLA/HNT10, and PLA/PEG5/HNT10, respectively, and Table 2 reports the data for $T_{50\%}$ (50% mass loss temperature) and T_{max} of all the samples. It can be seen from Fig. 8 that the single step degradation occurred for all the samples, with more than 80% mass loss occurring in between 340 and 370 °C.

Neat PLA and PLA/PEG films showed 10% mass degradation at 305 °C, while PLA/HNT and PLA/PEG/HNT had same degradation at higher temperature, i.e., at 325 °C and 343 °C, respectively, and this might be due to the high thermal stability of HNT [38, 39]. As shown in Fig. 8a and reported in Table 2, the presence of HNT in the PLA also increases the onset degradation temperature, thus increasing the $T_{50\%}$ temperature for the PLA/HNT10 and PLA/PEG5/HNT10. Also, the residual mass of the sample containing HNT is higher than the neat PLA. HNTs are inorganic materials, and its incorporation in PLA structure is expected to enhance the thermal stability by affecting the chain interactions of the PLA molecules [38, 40]. Therefore, the thermal degradation results indicate that PEG alone did not have any effect on the thermal stability of PLA, but the addition of HNT in the PLA/PEG films improves overall the thermal stability, and this might be due to the synergistic effect of HNT and PEG on the PLA.

Furthermore, Fig. 8b shows the DTG curve and the peak represents the temperature of the maximum degradation rate (T_{max}). For neat PLA film, T_{max}

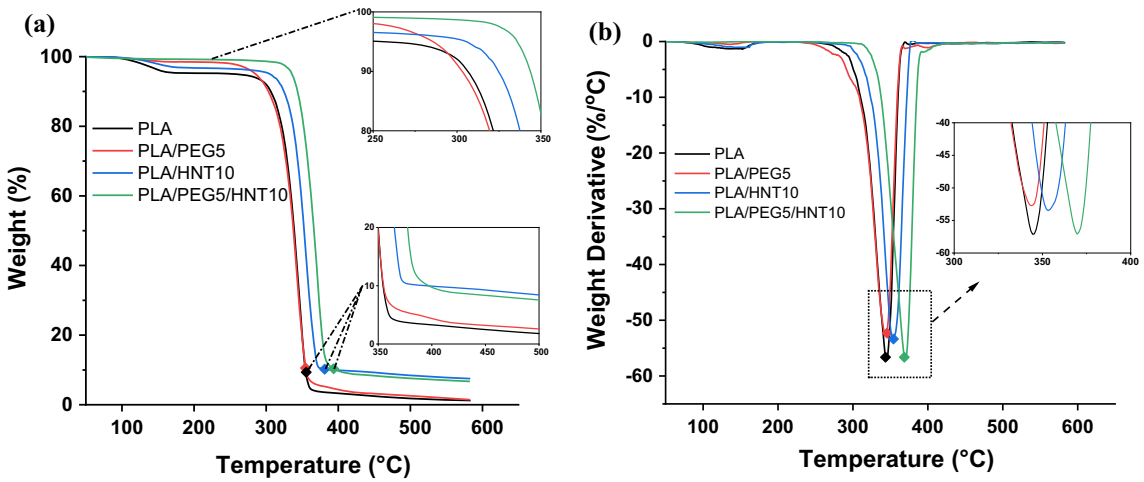

Figure 8 TGA (**a**) and DTG (**b**) curves of PLA and PLA composite films.

occurred at 346 °C, and no change in the T_{max} can be observed for the PLA/PEG5. However, the addition of HNT shifted the T_{max} to a higher temperature. The T_{max} for PLA/PEG5/HNT10 occurred at 370 °C, which is approximately 20 °C higher than the neat PLA, PLA/PEG5, and PLA/HNT10. Overall, the study indicates that the thermal stability of PLA increases due to the synergistic effect of PEG and HNT.

X-ray diffraction

X-ray diffraction study was conducted to study the effect of HNT and PEG-600 on the crystalline structure of the PLA. XRD scans of PLA, HNT, PLA/PEG5, PLA/HNT10, and PLA/PEG5/HNT10 are shown in Fig. 9. For as-received HNT powder, three major peaks appeared in XRD spectrograms at $2\theta = 11.85°$, 20.11°, and 24.96°, corresponding to reflection planes (001), (020), and (110,002) with d-spacing 0.746, 0.441, and 0.356, respectively [16, 19]. In the case of neat PLA, a broad scattering pattern can be seen, suggesting the amorphous phase centered at $2\theta = 16.52°$ corresponding to the plane (110/200) [36, 41]. As PLA films are prepared by solvent casting route, the evaporation of the solvent is so quick that there may be no time for polymer crystallization

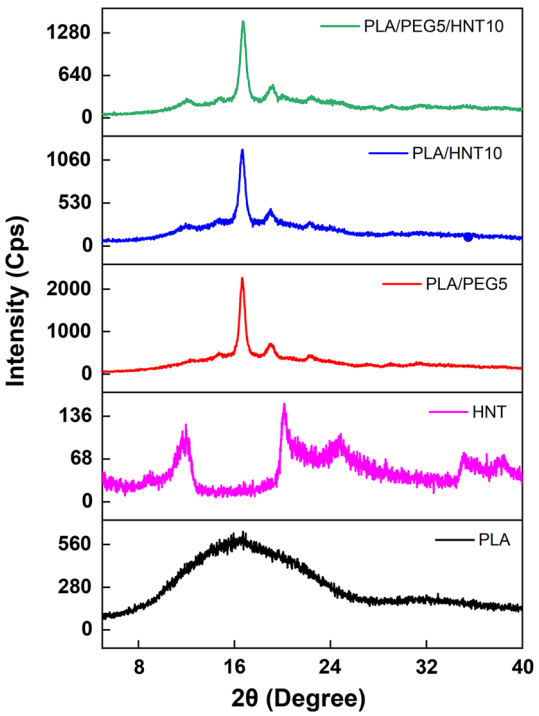

Figure 9 X-ray diffractograms of PLA and PLA composite films.

resulting in amorphous PLA. However, after the addition of HNT and PEG, the intensity of the PLA peak becomes stronger and sharper than the neat PLA matrix indicating an increase in crystallinity. Meanwhile, from the spectrograms, it is also evident that after addition of PEG and HNT, the 2θ peak of PLA corresponding to the plane (110/200) shifts toward the higher values of 2θ. Addition of PEG not only increased the chain mobility of PLA but also led to the formation of a more stable crystal structure [36]. The intensity of PLA/HNT peak is lower as compared to the peak intensity at PLA/PEG composite, suggesting lower crystallinity. PLA/PEG films show the highest crystallinity (32%) followed by PLA/PEG/HNT films which are 31.5% crystalline, whereas PLA/HNT films show the lowest crystallinity at 22.39%. The order of crystallinity obtained with XRD agrees with that obtained from DSC thermograms.

Conclusions

The neat PLA, PLA/PEG, PLA/HNT, and PLA/PEG/HNT composite films were prepared by solvent casting method, and their mechanical and thermal properties were analyzed. Tensile testing results revealed that the PEG acts as a plasticizer and improves the toughness of PLA by 1300% with 37% decrease in tensile strength at 5% PEG concentration. The addition of HNT in PLA did not affect the tensile strength at low concentration, but as the HNT content increased beyond 3 wt%, the tensile strength started to fall with increased brittleness. In the case of PLA/PEG5/HNT3 composite films, the tensile strength improved significantly as compared to plasticized PLA (PLA/PEG5). At higher concentrations of HNT, tensile strength decreases due to the agglomerations. Thermal analysis of the films showed a decrease in T_g in PLA/PEG film indicating the increased chain mobility due to the presence of plasticizer, while no change in T_g was observed in the case of PLA/HNT composite films. Also, the addition of PEG and HNT in PLA improves the degree of crystallinity which agreed with XRD analysis. Thermal stability of the films improved due to the addition of HNT in the PLA and PLA/PEG. Storage modulus significantly increases in the rubbery region for PLA/PEG and PLA/PEG/HNT when compared with neat PLA, and Tanδ peak showed a shift toward higher temperature

with broadening of peak after introduction of HNTs in the PLA and PLA/PEG films. This improvement in the storage modulus and Tan δ is due to the synergistic effect of PEG and HNT on the PLA.

References

[1] Liu X, Dever M, Fair N, Benson RS (1997) Thermal and mechanical properties of poly(lactic acid) and poly(ethylene/butylene succinate) blends. J Environ Polym Degrad 5:225–235. https://doi.org/10.1007/BF02763666

[2] Raquez J-M, Habibi Y, Murariu M, Dubois P (2013) Polylactide (PLA)-based nanocomposites. Prog Polym Sci 38:1504–1542. https://doi.org/10.1016/j.progpolymsci.2013.05.014

[3] Shah BL, Selke SE, Walters MB, Heiden PA (2008) Effects of wood flour and chitosan on mechanical, chemical, and thermal properties of polylactide. Polym Compos 29:655–663. https://doi.org/10.1002/pc.20415

[4] Auras R, Harte B, Selke S (2004) An overview of polylactides as packaging materials. Macromol Biosci 4:835–864. https://doi.org/10.1002/mabi.200400043

[5] Hassouna F, Raquez JM, Addiego F et al (2011) New approach on the development of plasticized polylactide (PLA): grafting of poly(ethylene glycol) (PEG) via reactive extrusion. Eur Polym J 47:2134–2144. https://doi.org/10.1016/j.eurpolymj.2011.08.001

[6] Kulinski Z, Piorkowska E, Gadzinowska K, Stasiak M (2006) Plasticization of poly(L-lactide) with poly(propylene glycol). Biomacromol 7:2128–2135. https://doi.org/10.1021/bm060089m

[7] Al-Mulla EAJ, Yunus WMZW, Ibrahim NAB, Rahman MZA (2010) Properties of epoxidized palm oil plasticized polytlactic acid. J Mater Sci 45:1942–1946. https://doi.org/10.1007/s10853-009-4185-1

[8] Jacobsen S, Fritz HG (1999) Plasticizing polylactide?the effect of different plasticizers on the mechanical properties. Polym Eng Sci 39:1303–1310. https://doi.org/10.1002/pen.11517

[9] Shi X, Zhang G, Phuong TV, Lazzeri A (2015) Synergistic effects of nucleating agents and plasticizers on the crystallization behavior of poly(lactic acid). Molecules 20:1579–1593. https://doi.org/10.3390/molecules20011579

[10] Mohapatra AK, Mohanty S, Nayak SK (2014) Effect of PEG on PLA/PEG blend and its nanocomposites: a study of thermo-mechanical and morphological characterization. Polym Compos 35:283–293. https://doi.org/10.1002/pc.22660

[11] Saura JJ, Gimenez E, Feijoo JL et al (2005) Development of amorphous PLA-montmorillonite nanocomposites. J Mater Sci 40:1785–1788. https://doi.org/10.1007/s10853-005-0694-8

[12] Frone AN, Panaitescu DM, Chiulan I et al (2016) The effect of cellulose nanofibers on the crystallinity and nanostructure of poly(lactic acid) composites. J Mater Sci 51:9771–9791. https://doi.org/10.1007/s10853-016-0212-1

[13] Zhou Y, Lei L, Yang B et al (2018) Preparation and characterization of polylactic acid (PLA) carbon nanotube nanocomposites. Polym Test 68:34–38. https://doi.org/10.1016/j.polymertesting.2018.03.044

[14] De Silva RT, Pasbakhsh P, Mae LS, Kit Y (2015) ZnO deposited/encapsulated halloysite-poly (lactic acid) (PLA) nanocomposites for high performance packaging films with improved mechanical and antimicrobial properties. Appl Clay Sci 111:10–20. https://doi.org/10.1016/j.clay.2015.03.024

[15] Zhang Y, Tang A, Yang H, Ouyang J (2016) Applications and interfaces of halloysite nanocomposites. Appl Clay Sci 119:8–17. https://doi.org/10.1016/j.clay.2015.06.034

[16] Liu M, Jia Z, Jia D, Zhou C (2014) Recent advance in research on halloysite nanotubes-polymer nanocomposite. Prog Polym Sci 39:1498–1525. https://doi.org/10.1016/j.progpolymsci.2014.04.004

[17] Bugatti V, Viscusi G, Naddeo C, Gorrasi G (2017) Nanocomposites based on PCL and halloysite nanotubes filled with lysozyme: effect of draw ratio on the physical properties and release analysis. Nanomater (Basel, Switzerland) 7:213. https://doi.org/10.3390/nano7080213

[18] Gorrasi G, Senatore V, Vigliotta G et al (2014) PET-halloysite nanotubes composites for packaging application: preparation, characterization and analysis of physical properties. Eur Polym J 61:145–156. https://doi.org/10.1016/j.eurpolymj.2014.10.004

[19] Dong Y, Marshall J, Haroosh HJ et al (2015) Polylactic acid (PLA)/halloysite nanotube (HNT) composite mats: influence of HNT content and modification. Compos PART A 76:28–36. https://doi.org/10.1016/j.compositesa.2015.05.011

[20] Esma C, Erpek Y, Ozkoc G, Yilmazer U (2016) Effects of halloysite nanotubes on the performance of plasticized poly(lactic acid)-based composites. Polym Compos 37:3134–3148. https://doi.org/10.1002/pc.23511

[21] Meng X, Nguyen NA, Tekinalp H et al (2017) Supertough PLA-silane nanohybrids by in situ condensation and grafting. ACS Sustain Chem Eng 6:1289–1298. https://doi.org/10.1021/acssuschemeng.7b03650

[22] Herrera N, Mathew AP, Oksman K (2015) Plasticized polylactic acid/cellulose nanocomposites prepared using

melt-extrusion and liquid feeding: mechanical, thermal and optical properties. Compos Sci Technol 106:149–155. https://doi.org/10.1016/j.compscitech.2014.11.012

[23] Suryanegara L, Nakagaito AN, Yano H (2009) The effect of crystallization of PLA on the thermal and mechanical properties of microfibrillated cellulose-reinforced PLA composites. Compos Sci Technol 69:1187–1192. https://doi.org/10.1016/j.compscitech.2009.02.022

[24] Majhi SK, Nayak SK, Mohanty S, Unnikrishnan L (2010) Mechanical and fracture behavior of banana fiber reinforced polylactic acid biocomposites. Int J Plast Technol 14:57–75. https://doi.org/10.1007/s12588-010-0010-6

[25] Pillin I, Montrelay N, Grohens Y (2006) Thermo-mechanical characterization of plasticized PLA: Is the miscibility the only significant factor? Polymer 47:4676–4682. https://doi.org/10.1016/j.polymer.2006.04.013

[26] Ozdemir E, Hacaloglu J (2017) Characterizations of PLA-PEG blends involving organically modified montmorillonite. J Anal Appl Pyrolysis 127:343–349. https://doi.org/10.1016/J.JAAP.2017.07.016

[27] Imsombut T, Srisa-Ard M, Baimark Y (2017) Synthesis of star-shaped ε-caprolactone oligomers for use as plasticizers of poly(L-lactide) bioplastic films. Orient J Chem 33:654–663. https://doi.org/10.13005/ojc/330213

[28] Bijarimi M, Ahmad S, Rasid R (2013) Mechanical, thermal and morphological properties of poly(lactic acid)/natural rubber nanocomposites. J Reinf Plast Compos 32:1656–1667. https://doi.org/10.1177/0731684413496487

[29] Wang B, Hina K, Zou H et al (2018) Thermal, crystallization, mechanical and decomposition properties of poly(lactic acid) plasticized with poly(ethylene glycol). J Vinyl Add Tech 24:E154–E163. https://doi.org/10.1002/vnl.21619

[30] Salas-Papayanopolos H, Morales-Cepeda AB, Sanchez S et al (2017) Synergistic effect of silver nanoparticle content on the optical and thermo-mechanical properties of poly(l-lactic acid)/glycerol triacetate blends. Polym Bull 74:4799–4814. https://doi.org/10.1007/s00289-017-1992-4

[31] Singh AA, Geng S, Herrera N, Oksman K (2018) Aligned plasticized polylactic acid cellulose nanocomposite tapes: effect of drawing conditions. Compos Part A Appl Sci Manuf 104:101–107. https://doi.org/10.1016/j.compositesa.2017.10.019

[32] Mohapatra AK, Mohanty S, Nayak SK (2014) Dynamic mechanical and thermal properties of polylactide-layered silicate nanocomposites. J Thermoplast Compos Mater 27:699–716. https://doi.org/10.1177/0892705712454446

[33] Giita Silverajah VS, Ibrahim NA, Yunus WMZW et al (2012) A comparative study on the mechanical, thermal and morphological characterization of poly(lactic acid)/epoxidized palm oil blend. Int J Mol Sci 13:5878–5898. https://doi.org/10.3390/ijms13055878

[34] Ahmed J, Varshney SK, Auras R, Hwang SW (2010) Thermal and rheological properties of L-polylactide/polyethylene glycol/silicate nanocomposites films. J Food Sci 75:N97–N108. https://doi.org/10.1111/j.1750-3841.2010.01809.x

[35] Rao YQ, Pochan JM (2007) Mechanics of polymer-clay nanocomposites. Macromolecules 40:290–296. https://doi.org/10.1021/ma061445w

[36] Li F-J, Zhang S-D, Liang J-Z, Wang J-Z (2015) Effect of polyethylene glycol on the crystallization and impact properties of polylactide-based blends. Polym Adv Technol 26:465–475. https://doi.org/10.1002/pat.3475

[37] Therias S, Murariu M, Dubois P (2017) Bionanocomposites based on PLA and halloysite nanotubes: from key properties to photooxidative degradation. Polym Degrad Stab 145:60–69. https://doi.org/10.1016/J.POLYMDEGRADSTAB.2017.06.008

[38] Liu M, Zhang Y, Zhou C (2013) Nanocomposites of halloysite and polylactide. Appl Clay Sci 75:52–59. https://doi.org/10.1016/j.clay.2013.02.019

[39] Lai S-M, Wu S-H, Lin G-G, Don T-M (2014) Macromolecular Nanotechnology Unusual mechanical properties of melt-blended poly(lactic acid) (PLA)/clay nanocomposites. Eur Polym J 52:193–206. https://doi.org/10.1016/j.eurpolymj.2013.12.012

[40] Cai N, Dai Q, Wang Z et al (2015) Toughening of electrospun poly(l-lactic acid) nanofiber scaffolds with unidirectionally aligned halloysite nanotubes. J Mater Sci 50:1435–1445. https://doi.org/10.1007/s10853-014-8703-4

[41] Russo V, Tammaro L, Di Marcantonio L et al (2016) Amniotic epithelial stem cell biocompatibility for electrospun poly(lactide-co-glycolide), poly(ε-caprolactone), poly(lactic acid) scaffolds. Mater Sci Eng C 69:321–329. https://doi.org/10.1016/J.MSEC.2016.06.092